Journal of Chemical Crystallography (2021) 51:394–404
https://doi.org/10.1007/s10870-020-00863-0

ORIGINAL PAPER

Structural Characterization of Two Polymorphs of 1-(4-Methylpyridin-2-yl)thiourea and Two Derived 2-Aminothiazoles

Denise Böck[1] · Andreas Beuchel[1] · Richard Goddard[2] · Peter Imming[1] · Rüdiger W. Seidel[1]

Received: 11 June 2020 / Accepted: 12 September 2020 / Published online: 1 October 2020

Abstract

Two polymorphic forms of 1-(4-methylpyridin-2-yl)thiourea (**1**) and the crystal and molecular structures of the 2-aminothiazoles *N*-(4-methylpyridin-2-yl)-4-(pyridin-2-yl)thiazol-2-amine (**2**) and *N*-(4-methylpyridin-2-yl)-4-(pyrazin-2-yl) thiazol-2-amine (**3**), derived from **1** and the respective α-bromoketone via the Hantzsch reaction, are described. Both polymorphic forms **1α** (space group $P2_1/c$, $Z=4$) and **1β** (space group $P2_1/n$, $Z=8$) crystallize in the monoclinic system but exhibit distinctly different intermolecular hydrogen bonding patterns. Compound **2** (orthorhombic, space group $Pca2_1$, $Z=8$) forms polymeric N–H···N hydrogen-bonded zigzag tapes in the polar crystal structure, with a significant twisting between the thiazole and pyridine rings. In contrast, the crystal structure of **3** (monoclinic, space group $P2_1/c$, $Z=4$) features nearly planar centrosymmetric N–H···N hydrogen-bonded dimers, which are laterally joined through long C–H···N contacts, affording a π···π stacked layered structure.

Graphic Abstract

Two polymorphs of 1-(4-methylpyridin-2-yl)thiourea and the crystal and molecular structures of two 2-aminothiazoles, derived from 1-(4-methylpyridin-2-yl)thiourea and α-bromoketones via Hantzsch reaction, are reported.

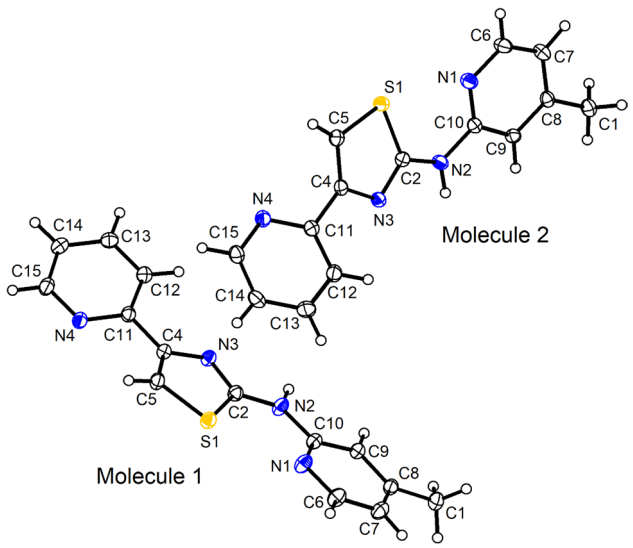

Keywords 1-(4-Methylpyridin-2-yl)thiourea · 2-Aminothiazoles · Hantzsch reaction · Hydrogen bonding · Polymorphism · Crystal structure

✉ Rüdiger W. Seidel
ruediger.seidel@pharmazie.uni-halle.de

Extended author information available on the last page of the article

Introduction

The 2-aminothiazole moiety is a synthetically flexible and pharmacologically promising scaffold in medicinal chemistry, and a number of drugs containing a 2-aminothiazole-4-subsituted moiety, e.g. cefdinir (antibiotic), mirabegron (β_3 adrenergic agonist) or the tyrosine kinase inhibitor dasatinib, are on the market. In recent years, anticancer, antiepileptic, neuroprotective, antidiabetic, antihypertensive, anti-inflammamory, antiviral, antibiotic and antileishmanial properties of 2-aminothiazoles were investigated [1].

N,4-Diaryl substituted 2-aminothiazoles were prepared based on one of the ten scaffolds with antileishmanial properties from a screening of 200,000 compounds [2]. Other microorganisms that are inhibited by this class of compounds include plasmodia [3] and mycobacteria [4]. For mycobacteria, the Tuberculosis Antimicrobial Acquisition and Coordinating Facility discovered an aminothiazole cluster of active compounds that formed the basis of an extensive structure–activity relationship (SAR) study [5]. Makam and Kannan showed that several substituted 2-aminothiazole derivatives exhibited antimycobacterial activity against *Mycobacterium tuberculosis*, $H_{37}Rv$, with minimum inhibitory concentration (MIC) values of 6.25–12.50 µM and proposed that these may be targeting the KasA protein in turn disturbing the cell wall biosynthesis by obstructing mycolic acid synthesis [6]. Another study explored structure–activity relationships for 2-aminothiazoles as potassium channel blockers [7], an undesirable pharmacological effect in most cases, which needs to be prevented by modification of the substitution pattern on the 2-aminothiazole moiety. While *N*-alkyl and *N*-aryl 2-aminothiazoles are distinguished by therapeutically very desirable acitivities, they are also known to be cytotoxic [5]. This is most likely due to the unsubstituted 5-position, which unspecifically engages in redox reactions in biochemical pathways. In the course of our ongoing investigations towards reduced toxicity of this compound class, we structurally characterized 2-aminothiazoles by X-ray crystallography to gain information on the conformational preferences in the solid-state. The extent of the conjugated system and the steric accessibility of the sulfur atom and 5-position is expected to have an influence on the stability, particularly with regard to oxidation.

Synthesis of 2-amino-4-substituted thiazoles can be accomplished via different routes [8]. Hantzsch synthesis from α-haloketones and thiourea derivatives in polar solvents is a general method [9, 10]. From 1-(4-methylpyridin-2-yl)thiourea (**1**) and the respective α-bromoketone, we synthesized the two 2-aminothiazoles *N*-(4-methylpyridin-2-yl)-4-(pyridin-2-yl)thiazol-2-amine (**2**) and *N*-(4-methylpyridin-2-yl)-4-(pyrazin-2-yl)thiazol-2-amine (**3**) through Hantzsch synthesis (Scheme 1). Compound **2** is contained in the Stasis Box (Medicines for Malaria Venture, MMV, Geneva, Switzerland) as MMV006357 and was identified as an antimycobacterial [4, 11] agent and potential drug candidate for eumycetoma [12]. Although coordination compounds bearing **2** as ligand were reported more than 40 years ago [13], to the best of our knowledge and based on a WebCSD search in June 2020 [14], small molecule crystal structures of **2**, its pyrazine derivative **3** and the starting thiourea derivative **1** have not been reported so far. Likewise, a search of the Protein Data Bank [15] yielded no structures containing **2** or **3** as ligands. Herein, we describe the structures of two polymorphs of **1**, henceforth named **1α** and **1β**, and the crystal and molecular structures of 2-aminothiazoles **2** and **3**, as determined by X-ray crystallography.

Experimental Section

General

Starting materials were purchased and used as received. Solvents were of analytical grade. The syntheses of 1-benzoyl-3-(4-methylpyridin-2-yl)thiourea [16] and 2-bromo-1-(pyridin-2-yl)ethanone hydrobromide [17] can be found in the literature.

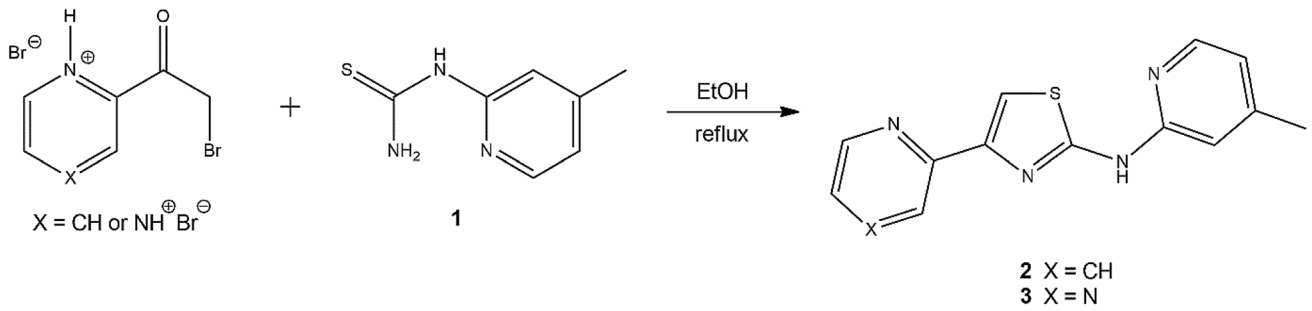

Scheme 1 Synthesis of aminothiazoles **2** and **3** from **1** and the respective α-bromoketone

Physical Methods

^{1}H and ^{13}C NMR spectra were recorded at room temperature on a Varian INOVA 500 NMR spectrometer. The residual solvent signals of DMSO-*d*6 ($\delta_{1H} = 2.50$ ppm, $\delta_{13C} = 39.51$ ppm) were used to reference the spectra (s = singlet, bs = broad singlet, d = doublet, dd = double doublet). The high-resolution mass spectrum was measured on a Bruker Daltonics Apex III FT-ICR mass spectrometer.

Synthesis and Crystallization

1-(4-Methylpyridin-2-yl)thiourea (1)

Compound **1** was synthesized by adapting a literature protocol [18]. 7.4 mL of 1 N aqueous NaOH were added to a stirred suspension of 1-benzoyl-3-(4-methylpyridin-2-yl)thiourea (2.00 g, 7.37 mmol) in 15 mL of methanol. The mixture was then heated to reflux for 1 h. After cooling to room temperature, a white solid formed, which was separated by filtration, washed with deionized water and dried over P_2O_5 in a vacuum desiccator to yield 1.00 g of **1** (5.98 mmol, 81%). Physical properties were in agreement with those reported in the literature [19]. Crystals of **1α** suitable for X-ray diffraction were obtained by recrystallization from methanol, and those of **1β** were grown from a solution in $CDCl_3$ by slow evaporation of the solvent.

N-(4-Methylpyridin-2-yl)-4-(pyridin-2-yl)thiazol-2-amine (2)

Compound **2** was synthesized following a modified literature procedure [20]. Compound **1** (83 mg, 0.50 mmol) and 2-bromo-1-(pyridin-2-yl)ethanone hydrobromide (140 mg, 0.50 mmol) were dissolved in 5 mL of ethanol and triethylamine (0.1 mL) was added. The reaction mixture was refluxed for 2 h. Subsequently, the solvent was removed using a rotary evaporator. The residue was taken up in 10 mL of a saturated K_2CO_3 solution and extracted three times with ethyl acetate. The combined organic layers were washed with brine and dried over $MgSO_4$. The solvent was removed under reduced pressure and the crude product recrystallized from methanol. Yield: 54 mg (0.20 mmol, 40%). Spectroscopic properties were in agreement with those reported in the literature [2, 20]. Crystals for X-ray diffraction were taken from the mother liquor.

N-(4-Methylpyridin-2-yl)-4-(pyrazin-2-yl)thiazol-2-amine (3)

Compound **3** was prepared in analogy to **2** from **1** and 2-bromo-1-(pyrazin-2-yl) ethanone hydrobromide [21] (note that the compound was not named hydrobromide by these authors), which was synthesized from acetylpyrazine (0.50 g, 4.00 mmol) using 2-pyrrolidinone hydrotribromide (2.18 g, 4.4 mol) as reagent and used in situ without purification. Yield (based on **1**): 75 mg (0.28 mmol, 7%). ^{1}H NMR (500 MHz, DMSO-*d*6): $\delta = 11.46$ (s, 1H), 9.14 (d, $J = 1.5$ Hz, 1H), 8.64 (dd, $J = 2.5$, 1,5 Hz, 1H), 8.55 (d, $J = 2.5$ Hz, 1H), 8.17 (d, $J = 5.2$ Hz, 1H), 7.75 (s, 1H), 6.89 (bs, 1H), 6.79 (dd, $J = 5.2$ Hz, 1H), 2.28 (s, 3H) ppm; ^{13}C NMR (126 MHz, DMSO-*d*6): $\delta = 160.5$, 151.8, 148.7, 147.7, 146.2, 146.0, 144.4, 143.3, 141.4, 117.7, 111.7, 110.7, 20.7 ppm. HRMS(ESI): calcd. for $C_{13}H_{11}N_5S$ $[M+H]^+$ 270.0813, found 270.0806. Crystals for X-ray diffraction were taken from the mother liquor.

Crystal Structure Determination

The X-ray intensity data for **1α** and **3** were measured on a Bruker AXS Apex II diffractometer, equipped respectively with an Incoatec IμS microfocus X-ray source and a FR591 rotating anode radiation source. The diffraction data for **2** were collected on an Enraf–Nonius KappaCCD diffractometer with a FR591 rotating anode. The SAINT software was used to perform data reductions [22]. The intensity measurements for **1β** were carried out on the P11 beamline at the PETRA III light source (DESY, Hamburg) at an X-ray energy of 22.0 keV. The primary beam intensity was monitored continuously and stored during the experiment. The P11 X-ray optics consisted of a liquid nitrogen-cooled Si(111) and Si(113) double-crystal monochromator and one vertical and two horizontal deflecting X-ray mirrors. The source brilliance at the crystal was 1.7×10^{12} photons per second. The data were collected using a 200 μm beam on a PILATUS 6 M-0109 detector (Dectris Ltd, Baden, Switzerland) [23] at a distance of 163.4 mm from the crystal. The 20-bit dynamic range of the PILATUS 6 M detector allowed for collection of weak high-order and stronger low-order reflections at the same time in one run. The crystal was rotated by 360° in steps of 0.5° with an exposure of 0.250 s per frame with a filter transmission of 0.1 using the P11 Crystallography Control graphical user interface at the P11 beamline [24]. The data were processed with the XDS program package [25]. Absorption corrections were carried out with SADABS [26].

The crystal structures were solved with SHELXT-2018/1 [27] and refined with SHELXL-2018/3 [28]. The structure of **1β** was refined using aspherical atomic scattering factors [29] and corrected for dispersion according to Kissel and Pratt [30]. Asphericity parameters were generated by the APEX3 software (IDEAL) [31]. Anisotropic displacement parameters were introduced for all non-hydrogen atoms. For **1α**, **2** and **3**, carbon-bound hydrogen atoms were placed at geometrically calculated positions with $C_{aromatic}$–H = 0.95 Å and C_{methyl}–H = 0.98 Å and refined with the appropriate riding model. Methyl groups were allowed to rotate to match the underlying electron density maxima. Hydrogen atoms

attached to nitrogen were localized in difference electron density maps and, for **1α**, **2** and **3**, refined with the N–H bond lengths restrained to a target value of 0.88(2) Å. U_{iso}(H) = 1.2 U_{eq}(C, N) (1.5 for methyl groups) was applied for all hydrogen atoms. Packing indices were calculated with PLATON [32]. Structure pictures were generated with Diamond [33] and Mercury [34]. Crystal data and refinement details for **1α**, **1β**, **2** and **3** are listed in Table 1.

Results and Discussion

Polymorphic Forms of 1

Two monoclinic crystal forms of **1** were encountered. **1α** with one molecule in the asymmetric unit ($Z'=1$) formed upon recrystallization from methanol, and **1β** with two crystallographically unique molecules ($Z'=2$) crystallized from a solution of the compound in $CDCl_3$. Figure 1 shows displacement ellipsoid plots of both structures, and Table 2 compares selected bond lengths and torsion angles. The bond lengths are comparable with those in the parent 1-(pyridine-2-yl)thiourea (CSD refcode: HIRPAA) [35]. Both **1α** and **1β** have in common a six-membered ring intramolecular N–H···N hydrogen bond between the primary amino group on the thiourea moiety and the pyridine nitrogen atom, which is in accord with Etter's second hydrogen bond rule for organic compounds, namely that six-membered ring intramolecular hydrogen bonds form in preference to intermolecular hydrogen bonds [36]. The graph-set assignment for this hydrogen bond motif is S(6). This requires a synperiplanar conformation between the pyridine nitrogen atom and the thiocarbonyl carbon atom C1, and likewise between the pivot carbon atom C2 of the pyridine ring and the primary amino group. The same intramolecular hydrogen bond and molecular conformation was found in HIRPAA. Like in HIRPAA, the molecule is virtually planar in **1α** (r.m.s. deviation 0.0234 Å for the non-hydrogen atoms). In contrast, the two unique molecules in **1β** deviate markedly from planarity by a tilt of the thiourea group from the plane of the pyridine ring, as revealed by the respective angles between the mean planes of the two groups [molecule 1: 14.16(5)°; molecule 2: 18.08(5)°] and the torsion angles listed in Table 2.

Table 1 Crystal data and refinement details for **1α**, **1β**, **2** and **3**

	1α	**1β**	**2**	**3**
Empirical formula	$C_7H_9N_3S$	$C_7H_9N_3S$	$C_{14}H_{12}N_4S$	$C_{13}H_{11}N_5S$
M_r	167.23	167.23	268.34	269.33
T (K)	100(2)	100(2)	100(2)	100(2)
λ (Å)	0.71073	0.6199	0.71073	1.54178
Crystal system	Monoclinic	Monoclinic	Orthorhombic	Monoclinic
Space group	$P2_1/c$ (No. 14)	$P2_1/n$ (No. 14)	$Pca2_1$ (No. 29)	$P2_1/c$ (No. 14)
a (Å)	6.9526(13)	8.2312(16)	7.3353(7)	7.3009(2)
b (Å)	14.473(3)	16.095(3)	26.7342(16)	15.5664(4)
c (Å)	8.1672(15)	12.240(3)	13.1949(9)	10.8403(3)
β (°)	102.395(4)	97.10(3)	90	96.320(1)
V (Å^3)	802.7(3)	1609.2(6)	2587.6(3)	1224.50(6)
Z, Z'	4, 1	8, 2	8, 2	4, 1
V/molecule (Å^3)	200.7	201.2	323.5	306.1
ρ_{calc} (g cm^{-3})	1.384	1.381	1.378	1.461
μ (mm^{-1})	0.337	0.230	0.241	2.290
F(000)	352	704	1120	560
Crystal size (mm)	0.168 × 0.106 × 0.021	0.156 × 0.103 × 0.091	0.170 × 0.120 × 0.110	0.223 × 0.196 × 0.120
θ range (°)	2.815–30.982	1.832–26.193	2.880–33.098	4.992–73.002
Reflections collected / unique	20,352 / 2538	30,415 / 4753	59,604 / 9807	42,832 / 2360
R_{int}	0.0642	0.0226	0.0542	0.0427
Observed reflections [$I > 2\sigma(I)$]	2109	4542	8482	2122
Goodness-of-fit on F^2	1.195	1.060	1.081	1.215
Parameters/restraints	110/3	256/0	359/3	176/1
R_1 [$I > 2\sigma(I)$]	0.0420	0.0248	0.0425	0.0410
wR_2 (all data)	0.1078	0.0702	0.1014	0.1129
$\Delta\rho_{max}$, $\Delta\rho_{min}$ (eÅ^{-3})	0.601, − 0.480	0.583, − 0.316	0.367, − 0.293	0.278, − 0.405

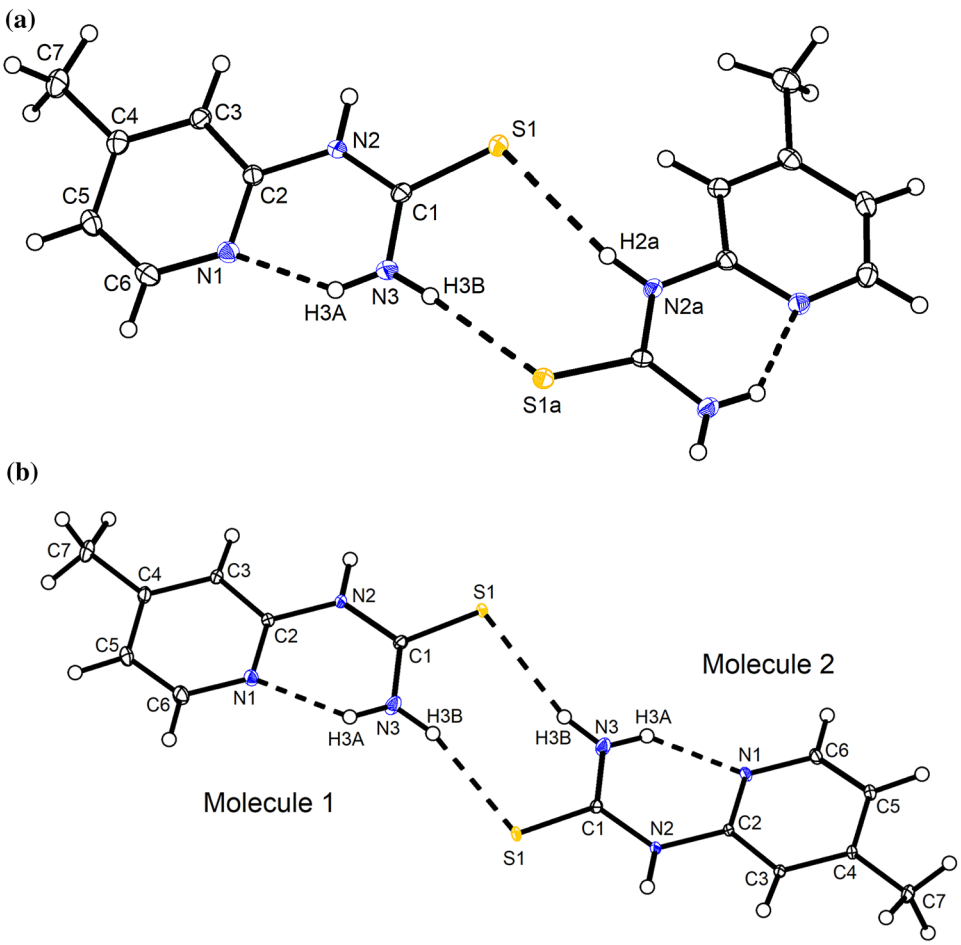

Fig. 1 **a** Hydrogen-bonded association of two symmetry-related molecules in **1α** and **b** of the two crystallographically distinct molecules in **1β**. Symmetry code: (a) x, 0.5 − y, 0.5 + z. Displacement ellipsoids are drawn at the 50% probability level. Hydrogen atoms are shown as small spheres of arbitrary radii. Dashed lines represent hydrogen bonds

Table 2 Selected bond lengths (Å) and torsion angles (°) for **1α** and **1β**

	1α	**1β**	
		Molecule 1	Molecule 2
C1–S1	1.7011(17)	1.7038(7)	1.7047(7)
C1–N2	1.355(2)	1.3634(9)	1.3644(8)
C1–N3	1.322(2)	1.3206(9)	1.3228(9)
C2–N2	1.403(2)	1.4045(8)	1.4069(8)
N1–C2–N2–C1	2.5(3)	17.0(1)	− 19.48(10)
N3–C1–N2–C2	− 2.8(3)	− 9.36(11)	15.49(10)

1α and **1β** exhibit distinctly different intermolecular hydrogen bonding patterns. Two self-complementary N–H···S hydrogen bonding sites on each molecule, provided by the sulfur atom as hydrogen bond acceptor and each of the primary and secondary amino groups as hydrogen bond donor sites, can lead to three possible combinations with $R_2^2(8)$ motifs (Scheme 2) [37]. As shown in Fig. 1, **1α** exhibits the asymmetric combination involving primary and secondary amino groups (type I), whereas **1β** shows the symmetric combination formed solely by the primary amino groups (type II). Type I is also observed for the structure of HIRPAA. Table 3 lists geometric parameters of the hydrogen bonds in **1α** and **1β**, which are as expected [35]. In **1α**, this hydrogen bond arrangement results in polymeric tapes extending through glide symmetry in the [001] direction (Fig. 2). In contrast, the secondary amino groups in **1β** are directed towards sulfur atoms of adjacent hydrogen-bonded dimers in the crystal structure with N···S distances of ca. 3.4 Å and significantly smaller H···S–C angles than in **1α**. The symmetric dimer in **1β** exhibits local inversion symmetry in the crystal structure. Frustration between competing intermolecular interactions, such as hydrogen bonds, and close packing has been put forward as a possible explanation for the $Z' > 1$ phenomenon [38]. The crystal structures of both **1α** and **1β** belong to the same space group type (No. 14), which is available for densest packing of molecules of arbitrary shape. The packing index is 69.6% for **1α** and 70.4% for **1β**, revealing a dense crystal packing in both forms [39]. It is worth noting that in spite of the different hydrogen bonding patterns, the calculated crystallographic density is almost the same for **1α** and **1β** (Table 1).

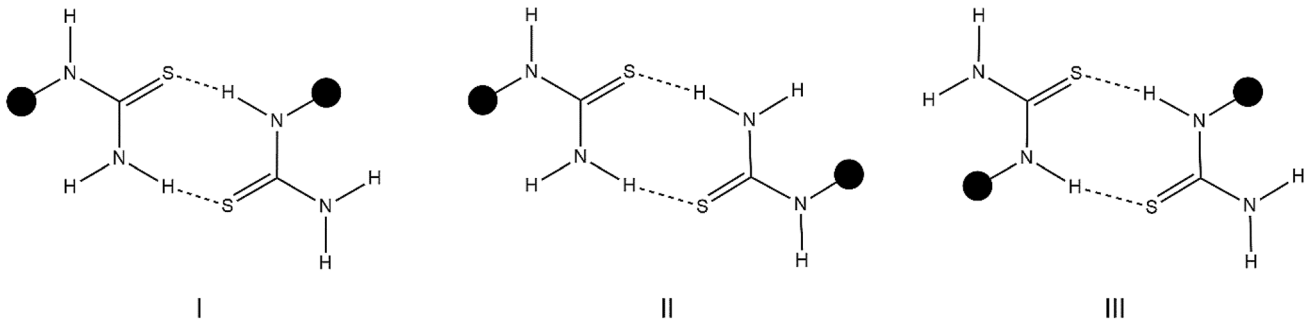

Scheme 2 Possible N–H···S hydrogen bond associations of **1** (the black circle represents 4-methylpyridin-2-yl) with $R_2^2(8)$ motifs. **1α** exhibits type I and **1β** shows type II. Type III is not seen here

Table 3 Hydrogen bond parameters (Å, °) for **1α** and **1β**

	d(*D*–*H*)	*d*(*H*···*A*)	*d*(*D*···*A*)	< (*DHA*)
1α[a]				
N2–H2···S1a	0.880(15)	2.462(16)	3.3324(15)	170(2)
N3–H3A···N1	0.873(16)	1.961(19)	2.670(2)	137(2)
N3–H3B···S1b	0.872(15)	2.485(16)	3.3553(16)	175(2)
1β[b]				
N31–H31A···N11	0.889(12)	1.990(11)	2.6844(10)	134.0(10)
N31–H31B···S12	0.922(12)	2.443(12)	3.3425(10)	165.1(10)
N32–H32A···N12	0.897(12)	1.994(11)	2.6970(9)	134.2(10)
N32–H32B···S11	0.913(11)	2.507(11)	3.3977(9)	165.0(9)

[a]Symmetry codes: (a) x, − y + 1/2, z − 1/2; (b) x, − y + 1/2, z + 1/2

[b]The second integer indicates unique molecule 1 or 2 (*cf.* Fig. 1)

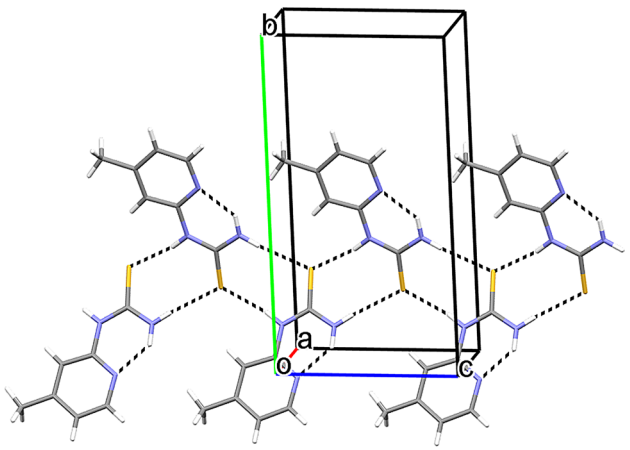

Fig. 2 Part of the crystal structure of **1α**, showing hydrogen-bonded tapes of the molecules extending parallel to the crystallographic *c* axis

Crystal and Molecular Structures of 2 and 3

Compound **2** crystallizes with two molecules in the asymmetric unit (Z′ = 2), as shown in Fig. 3. Selected bond lengths, bond angles and torsion angles are given in Table 4. In both molecules the thiazole sulfur atom S1 and the pivot carbon atom C10 of the pyridine ring as well as the pivot carbon atom of the thiazole ring C2 and the picoline nitrogen atom N1 are in a synperiplanar arrangement. The intramolecular N1···S1 distance is ca. 2.8 Å in both molecules and the C5–S1···N1 angles are 161.5 and 160.1° in molecule 1 and 2, respectively. From the structural point of view, this can be interpreted as chalcogen bonds between the picoline nitrogen lone pairs and the σ hole at the sulfur atoms opposite to the C5–S1 σ bonds [40, 41]. Interestingly, all 15 crystal structures of 2-aminothiazoles with *N*-bonded heteroaromatic substituents containing a nitrogen atom in the 2-position in the Cambridge Structural Database (June 2020) [42] exhibit planar conformations with intramolecular N···S distances of 2.70(4) Å (mean) in spite of different crystal environments, including structures of dasatinib and nine of its solvates [43, 44], as well as thiazovivin, a small molecule tool for stem cell research [45]. In contrast, 41 crystal structures of 2-aminothiazoles with variously substituted *N*-phenyl groups contain molecules in which the two moieties are randomly orientated to one another. The absence of any classical or weak hydrogen bonds towards the picoline nitrogen N1 corroborates this view. The dihedral angles between the mean planes through the thiazole rings and those through the pyridine rings attached to C4 is 22.96(8)° for molecule 1 and 37.53(6)° for molecule 2. Both molecules are thus significantly non-planar in this region. Clearly, the tilt between the pyridine ring and the thiazole ring should be disadvantageous for π electron delocalisation, but appears to be outweighed by the formation of strong intermolecular N–H···N hydrogen bonds between the amino group and the pyridine nitrogen atom N4 in the solid-state (Table 5). Molecule 1 and molecule 2 each form distinct hydrogen-bonded zigzag tapes extending in the [001] direction through glide symmetry (Fig. 4), resulting in a polar *c* axis. The packing index is 69.0%.

Figure 5 shows the molecular structure of **3**, bearing a pyrazinyl group at C4 of the thiazole ring instead of a

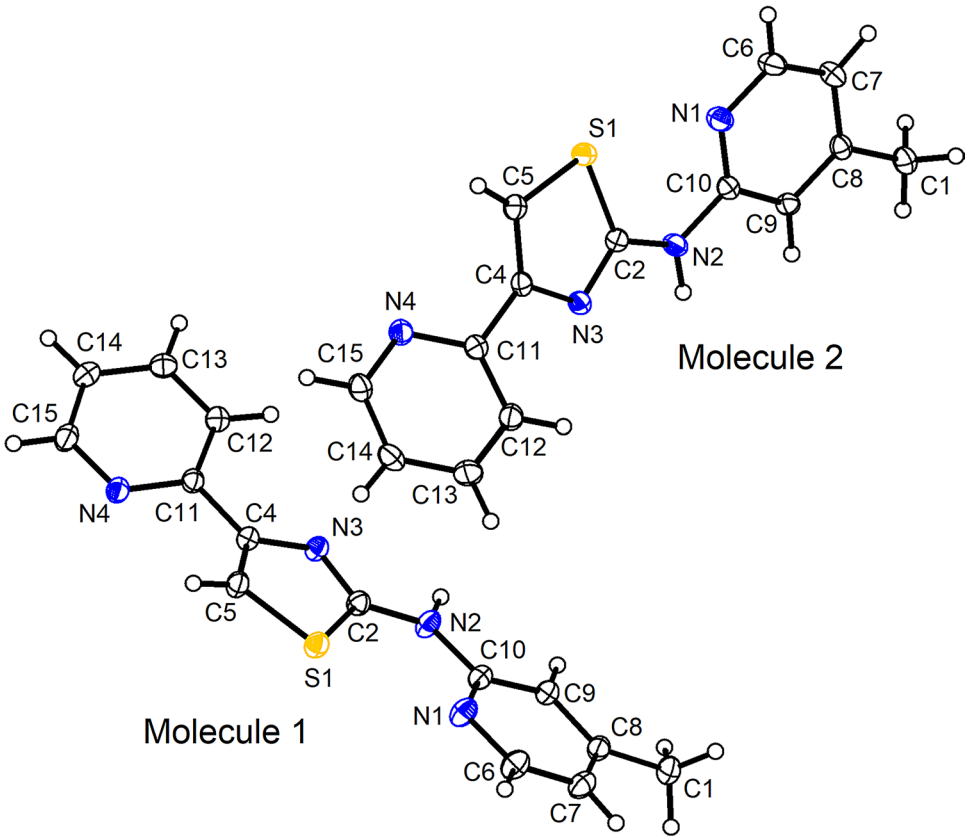

Fig. 3 Asymmetric unit of **2**. Displacement ellipsoids are drawn at the 50% probability level. Hydrogen atoms are shown as small spheres of arbitrary radii

Table 4 Selected bond lengths, bond angles and torsion angles (Å, °) for **2** and **3**

	2		**3**
	Molecule 1	Molecule 2	
C2–N3	1.312(3)	1.312(3)	1.309(2)
C2–N2	1.363(3)	1.370(3)	1.367(2)
C2–S1	1.748(2)	1.744(2)	1.7480(17)
C4–C5	1.362(3)	1.363(3)	1.355(2)
C4–N3	1.379(3)	1.379(3)	1.389(2)
C4–C11	1.473(3)	1.478(3)	1.469(2)
C5–S1	1.732(2)	1.724(2)	1.7212(17)
N3–C2–S1	114.94(17)	115.00(17)	115.31(13)
C5–C4–N3	115.9(2)	115.7(2)	115.85(15)
C4–C5–S1	110.21(17)	110.39(18)	110.68(13)
C5–S1–C2	88.6(1)	88.67(11)	88.48(8)
C2–N3–C4	110.4(2)	110.25(19)	109.67(14)
S1–C2–N2–C10	– 4.2(4)	14.8(3)	7.2(2)
N1–C10–N2–C2	– 1.6(4)	– 4.3(3)	– 1.2(2)
C5–C4–C11–N4	– 22.4(3)	37.4(3)	– 5.6(3)
N3–C4–C11–C12	– 23.3(3)	36.7(3)	– 8.0(3)

Table 5 Hydrogen bond parameters (Å, °) for **2** and **3**

	d(*D*–H)	*d*(H···*A*)	*d*(*D*···*A*)	< (*DHA*)
2[a]				
N21–H2_1…N41a	0.88(2)	2.01(2)	2.893(3)	177(3)
N22–H2_2…N42b	0.88(2)	2.10(2)	2.979(3)	177(3)
3[b]				
N2–H2…N5a	0.878(15)	2.053(15)	2.928(2)	174.2(19)
C6–H6…N4b	0.95	2.98	3.906(2)	165

[a] The second integer indicates unique molecule 1 or 2 (*cf.* Fig. 3). Symmetry codes: (a) – x + 1/2, y, z + 1/2; (b) – x + 3/2, y, z + 1/2

[b] Symmetry codes: (a) – x + 1, – y, – z; (b) – x + 2, – y, – z + 1

2-pyridinyl group as in **2**. Selected bond lengths, bond angles and torsion angles are listed in Table 4. Like **2**, the thiazole sulfur atom S1 and the pivot carbon atom C10 of the pyridine ring as well as the pivot carbon atom of the thiazole ring C2 and the picoline nitrogen atom N1 in **3** are in a synperiplanar orientation with an intramolecular S1···N1 distance of ca. 2.7 Å with a C5–S1···N1 angle of 162.5°. Thus, the observed conformation appears to be a characteristic trait of the *N*-(4-methylpyridin-2-yl) thiazol-2-amine moiety and is possibly supported by an intramolecular chalcogen bond (vide supra). In contrast to **2**, the dihedral angle between the mean plane through the thiazole ring and that through the pyrazin ring attached to C4 is only 7.25(6)°. The supramolecular structure of **3** in the crystal is distinctly different from that in **2**. Instead

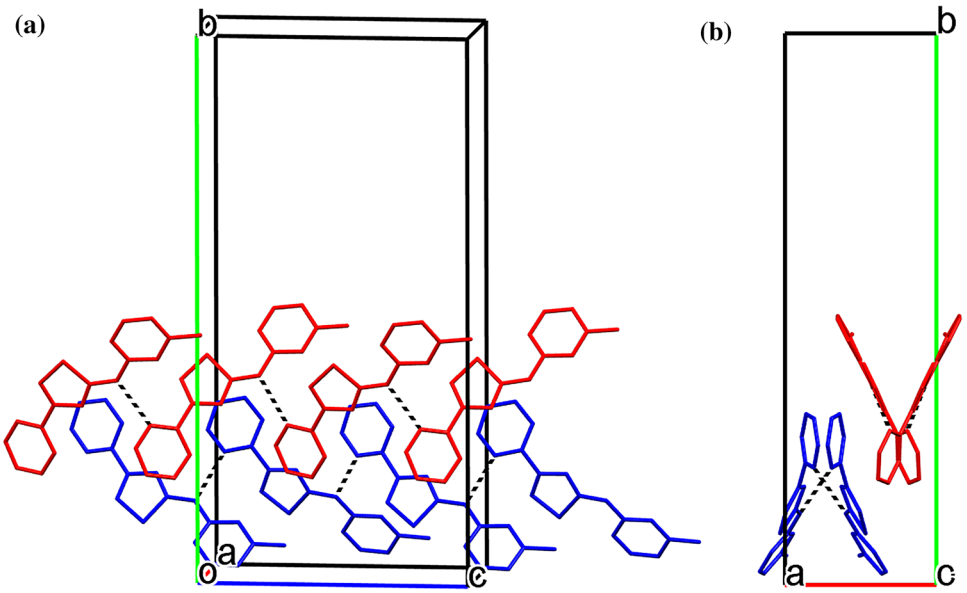

Fig. 4 Part of the crystal structure of **2**, viewed approximately along the *a* axis direction and **b** along the *c* axis direction. Hydrogen atoms have been omitted for clarity. Dashed lines represent hydrogen bonds. Red and blue colour indicate distinct hydrogen-bonded tapes resulting from unique molecules 1 and 2, respectively (*cf.* Fig. 3)

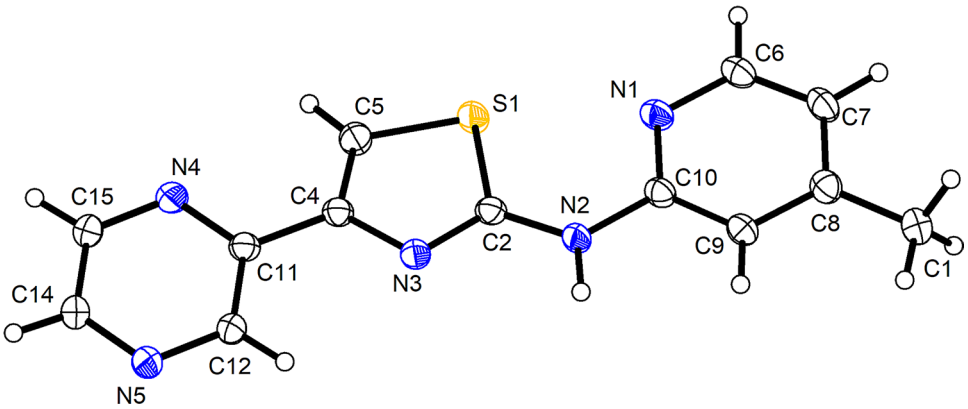

Fig. 5 Molecular structure of **3** in the crystal. Displacement ellipsoids are drawn at the 50% probability level. Hydrogen atoms are represented by small spheres of arbitrary radii

of the polymeric N–H···N hydrogen-bonded assemblies observed in **2**, the crystal structure of **3** is characterized by centrosymmetric dimers (Fig. 6). The amino group of each molecule forms a hydrogen bond to the pyrazine nitrogen atom in *meta* position to the thiazole ring, affording a $R_2^2(16)$ motif. The dimers so formed are laterally connected via C–H···N interactions involving the opposite pyrazine nitrogen atom. Although the H···*A* distance is longer than the sum of the van der Waals radii, the < (*DHA*) angle (Table 5) supports the presence of weak cooperative C–H···N hydrogen bonds [46]. The N–H···N hydrogen bonds and long C–H···N contacts generate layers of molecules parallel to (10–1), which are π···π stacked in the third dimension. The packing index for **3** of 71.4% reveals a denser crystal packing than in **2**. Since **2** and **3** differ only by one heteroatom site, it is possible that the weak cooperative C–H···N hydrogen bonds in **3** may have a structure-directing influence.

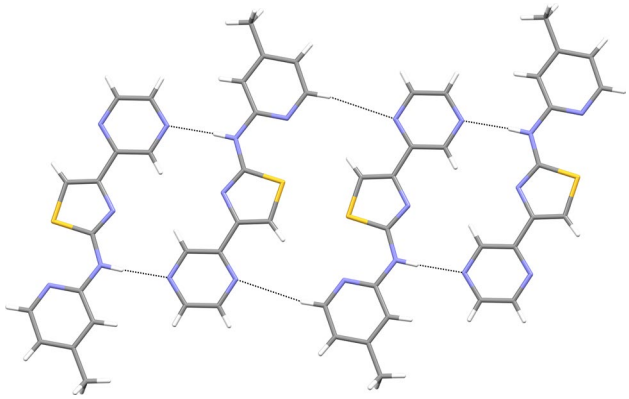

Fig. 6 Part of the crystal structure of **3**, viewed towards plane (10–1), showing two adjacent N–H···N hydrogen-bonded dimers laterally connected via long C–H···N contacts. Hydrogen bonds are shown by dashed lines

Conclusions

We synthesized two pharmacologically relevant *N*,4-diaryl substituted 2-aminothiazoles via Hantzsch synthesis and elucidated their structures. Structural characterization of the starting thiourea derivative **1** revealed two crystalline forms, which exhibit distinctly different intermolecular N–H···S hydrogen bonding patterns. For 2-aminothiazoles **2** and **3**, the encountered synperiplanar conformation of the *N*-(4-methylpyridin-2-yl)thiazol-2-amine moiety suggests the existence of supportive intramolecular N···S chalcogen bonds. Replacement of a pyridyl group in **2** by a pyrazinyl group in **3** has a significant effect on the supramolecular structures of **2** and **3** in the solid-state. Whereas **2** forms polymeric N–H···N hydrogen-bonded tapes, **3** forms N–H···N hydrogen-bonded cyclic dimers, which may further associate by additional weak intermolecular C–H···N hydrogen bonds. Since the number of structurally characterized *N*,4-diaryl substituted 2-aminothiazoles is hitherto limited, the structural insight gained from this study provides impetus for further exploration of this compound class in medicinal chemistry.

Supplementary Material

CCDC 2008777–2008780 contain the supplementary crystallographic data for this paper. These data can be obtained free of charge from the Cambridge Crystallographic Data Centre via www.ccdc.cam.ac.uk/structures.

Acknowledgements We acknowledge DESY (Hamburg, Germany), a member of the Helmholtz Association HGF, for the provision of experimental facilities. Parts of this research were carried out at the light source PETRA III and we would like to thank Dr Sofiane Saouane for assistance in using the beamline P11. Professor Christian W. Lehmann is gratefully acknowledged for his support of this project.

Author Contributions DB and AB synthesized the compounds studied and helped with the preparation of the manuscript. RG measured the X-ray diffraction data, solved the crystal structures and edited the manuscript. PI supervised the project and edited the manuscript. RWS refined the crystal structures and wrote the manuscript.

Funding Open Access funding enabled and organized by Projekt DEAL.

Data Availability Supplementary crystallographic data including reflection files have been deposited with the Cambridge Crystallographic Data Centre.

Compliance with Ethical Standards

Conflict of interest There are no conflicts of interest/competing interests to declare.

Informed Consent All authors have seen the manuscript and agree to its publication.

References

1. Das D, Sikdar P, Bairagi M (2016) Recent developments of 2-aminothiazoles in medicinal chemistry. Eur J Med Chem 109:89–98. https://doi.org/10.1016/j.ejmech.2015.12.022
2. Bhuniya D, Mukkavilli R, Shivahare R, Launay D, Dere RT, Deshpande A, Verma A, Vishwakarma P, Moger M, Pradhan A, Pati H, Gopinath VS, Gupta S, Puri SK, Martin D (2015) Aminothiazoles: Hit to lead development to identify antileishmanial agents. Eur J Med Chem 102:582–593. https://doi.org/10.1016/j.ejmech.2015.08.013
3. Paquet T, Gordon R, Waterson D, Witty MJ, Chibale K (2012) Antimalarial aminothiazoles and aminopyridines from phenotypic whole-cell screening of a SoftFocus® library. Fut Med Chem 4(18):2265–2277. https://doi.org/10.4155/fmc.12.176
4. Kesicki EA, Bailey MA, Ovechkina Y, Early JV, Alling T, Bowman J, Zuniga ES, Dalai S, Kumar N, Masquelin T, Hipskind PA, Odingo JO, Parish T (2016) Synthesis and evaluation of the 2-aminothiazoles as anti-tubercular agents. PLoS ONE 11(5):e0155209. https://doi.org/10.1371/journal.pone.0155209
5. Meissner A, Boshoff HI, Vasan M, Duckworth BP, Barry CE 3rd, Aldrich CC (2013) Structure-activity relationships of 2-aminothiazoles effective against Mycobacterium tuberculosis. Bioorg Med Chem 21(21):6385–6397. https://doi.org/10.1016/j.bmc.2013.08.048
6. Makam P, Kannan T (2014) 2-Aminothiazole derivatives as antimycobacterial agents: Synthesis, characterization, in vitro and in silico studies. Eur J Med Chem 87:643–656. https://doi.org/10.1016/j.ejmech.2014.09.086
7. Gentles RG, Grant-Young K, Hu S, Huang Y, Poss MA, Andres C, Fiedler T, Knox R, Lodge N, Weaver CD, Harden DG (2008) Initial SAR studies on apamin-displacing 2-aminothiazole blockers of calcium-activated small conductance potassium channels. Bioorg Med Chem Lett 18(19):5316–5319. https://doi.org/10.1016/j.bmcl.2008.08.023
8. Khalifa ME (2018) Recent developments and biological activities of 2-aminothiazole derivatives. Acta Chim Slov 65(1):1–22. https://doi.org/10.17344/acsi.2017.3547
9. Hantzsch A, Weber JH (1887) Ueber Verbindungen des Thiazols (Pyridins der Thiophenreihe). Ber Dtsch Chem Ges 20(2):3118–3132. https://doi.org/10.1002/cber.188702002200
10. Wang Z (2010) Hantzsch thiazole synthesis. In: Comprehensive organic name reactions and reagents, pp 1330–1334. https://doi.org/10.1002/9780470638859.conrr296
11. Grant SS, Kawate T, Nag PP, Silvis MR, Gordon K, Stanley SA, Kazyanskaya E, Nietupski R, Golas A, Fitzgerald M, Cho S, Franzblau SG, Hung DT (2013) Identification of novel inhibitors

of nonreplicating mycobacterium tuberculosis using a carbon starvation model. ACS Chem Biol 8(10):2224–2234. https://doi.org/10.1021/cb4004817
12. Lim W, Melse Y, Konings M, Phat Duong H, Eadie K, Laleu B, Perry B, Todd MH, Ioset J-R, van de Sande WWJ (2018) Addressing the most neglected diseases through an open research model: the discovery of fenarimols as novel drug candidates for eumycetoma. PLOS Neglect Trop Dis 12(4):e0006437. https://doi.org/10.1371/journal.pntd.0006437
13. Goodwin H, Mather D (1972) Anomalous magnetism of iron(II) complexes of methyl-substituted pyridylthiazoles. Aust J Chem 25(4):715–727. https://doi.org/10.1071/CH9720715
14. Thomas IR, Bruno IJ, Cole JC, Macrae CF, Pidcock E, Wood PA (2010) WebCSD: the online portal to the Cambridge Structural Database. J Appl Crystallogr 43:362–366. https://doi.org/10.1107/s0021889810000452
15. Burley SK, Berman HM, Bhikadiya C, Bi C, Chen L, Di Costanzo L, Christie C, Dalenberg K, Duarte JM, Dutta S, Feng Z, Ghosh S, Goodsell DS, Green RK, Guranovic V, Guzenko D, Hudson BP, Kalro T, Liang Y, Lowe R, Namkoong H, Peisach E, Periskova I, Prlic A, Randle C, Rose A, Rose P, Sala R, Sekharan M, Shao C, Tan L, Tao YP, Valasatava Y, Voigt M, Westbrook J, Woo J, Yang H, Young J, Zhuravleva M, Zardecki C (2019) RCSB Protein Data Bank: biological macromolecular structures enabling research and education in fundamental biology, biomedicine, biotechnology and energy. Nucleic Acids Res 47(D1):D464–D474. https://doi.org/10.1093/nar/gky1004
16. Saad FA (2014) Synthesis, spectral, electrochemical and X-ray single crystal studies on Ni(II) and Co(II) complexes derived from 1-benzoyl-3-(4-methylpyridin-2-yl) thiourea. Spectrochim Acta A 128:386–392. https://doi.org/10.1016/j.saa.2014.02.189
17. Cuconati A, Xu X, Block TM (2013) Preparation of substituted aminothiazoles as inhibitors of cancers, including hepatocellular carcinoma, and as inhibitors of hepatitis virus replication. WO2013052613A1
18. Amberg W, Netz A, Kling A, Ochse M, Lange U, Hutchins CW, Garcia-Ladona FJ, Wernet W (2007) Preparation of *N*-pyridin-2-ylguanidines and related compounds as 5-$_{HT}$5 receptor inhibitors. WO2007022964A2
19. Gallardo-Godoy A, Gever J, Fife KL, Silber BM, Prusiner SB, Renslo AR (2011) 2-Aminothiazoles as therapeutic leads for prion diseases. J Med Chem 54(4):1010–1021. https://doi.org/10.1021/jm101250y
20. Hung D, Serrano-Wu M, Grant S, Kawate T (2016) Substituted aminothiazoles for the treatment of tuberculosis. US20160031874A1
21. Dicks JP, Zubair M, Davies ES, Garner CD, Schulzke C, Wilson C, McMaster J (2015) Synthesis, structure and redox properties of asymmetric (Cyclopentadienyl)(ene-1,2-dithiolate)cobalt(III) complexes containing phenyl, pyridyl and pyrazinyl units. Eur J Inorg Chem 21:3550–3561. https://doi.org/10.1002/ejic.201500138
22. SAINT (2012) Bruker AXS Inc., Madison, Wisconsin, USA
23. Kraft P, Bergamaschi A, Broennimann C, Dinapoli R, Eikenberry EF, Henrich B, Johnson I, Mozzanica A, Schleputz CM, Willmott PR, Schmitt B (2009) Performance of single-photon-counting PILATUS detector modules. J Synchrot Radiat 16:368–375. https://doi.org/10.1107/s0909049509009911
24. Burkhardt A, Pakendorf T, Reime B, Meyer J, Fischer P, Stube N, Panneerselvam S, Lorbeer O, Stachnik K, Warmer M, Rodig P, Gories D, Meents A (2016) Status of the crystallography beamlines at PETRA III. Eur Phys J Plus 131(3):1–9. https://doi.org/10.1140/epjp/i2016-16056-0
25. Kabsch W (2010) XDS. Acta Crystallogr D 66:125–132. https://doi.org/10.1107/s0907444909047337
26. SADABS (2012) Bruker AXS Inc., Madison, Wisconsin, USA
27. Sheldrick GM (2015) SHELXT—integrated space-group and crystal-structure determination. Acta Crystallogr A 71(Pt 1):3–8. https://doi.org/10.1107/S2053273314026370
28. Sheldrick GM (2015) Crystal structure refinement with SHELXL. Acta Crystallogr C 71(Pt 1):3–8. https://doi.org/10.1107/S2053229614024218
29. Lübben J, Wandtke CM, Hübschle CB, Ruf M, Sheldrick GM, Dittrich B (2019) Aspherical scattering factors for SHELXL—model, implementation and application. Acta Crystallogr A 75(Pt 1):50–62. https://doi.org/10.1107/S2053273318013840
30. Kissel L, Pratt RH (1990) Corrections to tabulated anomalous-scattering factors. Acta Crystallogr Sect A 46(3):170–175. https://doi.org/10.1107/S0108767389010718
31. APEX3 (2018) Bruker AXS Inc., Madison, Wisconsin, USA
32. Spek AL (2020) checkCIF validation ALERTS: what they mean and how to respond. Acta Crystallogr E 76(Pt 1):1–11. https://doi.org/10.1107/S2056989019016244
33. Brandenburg K (2018) DIAMOND. 3.2k3 edn. Crystal Impact GbR, Bonn, Germany
34. Macrae CF, Sovago I, Cottrell SJ, Galek PTA, McCabe P, Pidcock E, Platings M, Shields GP, Stevens JS, Towler M, Wood PA (2020) Mercury 4.0: from visualization to analysis, design and prediction. J Appl Crystallogr 53 (Pt 1):226–235. https://doi.org/10.1107/S1600576719014092
35. Tutughamiarso M, Bolte M (2007) 1-(Pyridin-2-yl)thiourea. Acta Crystallogr E 63(12):o4682–o4682. https://doi.org/10.1107/s1600536807057388
36. Etter MC (1990) Encoding and decoding hydrogen-bond patterns of organic-compounds. Acc Chem Res 23(4):120–126. https://doi.org/10.1021/ar00172a005
37. Bernstein J, Davis RE, Shimoni L, Chang NL (1995) Patterns in hydrogen bonding—functionality and graph set analysis in crystals. Angew Chem-Int Edit 34(15):1555–1573. https://doi.org/10.1002/anie.199515551
38. Steed KM, Steed JW (2015) Packing problems: high Z' crystal structures and their relationship to cocrystals, inclusion compounds, and polymorphism. Chem Rev 115(8):2895–2933. https://doi.org/10.1021/cr500564z
39. Kitajgorodskij AI (1973) Molecular crystals and molecules. Academic Press, New York
40. Scilabra P, Terraneo G, Resnati G (2019) The chalcogen bond in crystalline solids: a world parallel to halogen bond. Acc Chem Res 52(5):1313–1324. https://doi.org/10.1021/acs.accounts.9b00037
41. Vogel L, Wonner P, Huber SM (2019) Chalcogen bonding: an overview. Angew Chem Int Ed 58(7):1880–1891. https://doi.org/10.1002/anie.201809432
42. Groom CR, Bruno IJ, Lightfoot MP, Ward SC (2016) The cambridge structural database. Acta Crystallogr B 72(Pt 2):171–179. https://doi.org/10.1107/S2052520616003954
43. Roy S, Quinones R, Matzger AJ (2012) Structural and physicochemical aspects of dasatinib hydrate and anhydrate phases. Cryst Growth Des 12(4):2122–2126. https://doi.org/10.1021/cg300152p
44. Sarcevica I, Grante I, Belyakov S, Rekis T, Berzins K, Actins A, Orola L (2016) Solvates of dasatinib: diversity and isostructurality. J Pharm Sci 105(4):1489–1495. https://doi.org/10.1016/j.xphs.2016.01.024
45. Ries O, Granitzka M, Stalke D, Ducho C (2013) Concise synthesis and X-ray crystal structure of *N*-Benzyl-2-(pyrimidin-4′-ylamino)-thiazole-4-carboxamide (Thiazovivin), a small-molecule tool for stem cell research. Synth Commun 43(21):2876–2882. https://doi.org/10.1080/00397911.2012.745567

46. Thakuria R, Sarma B, Nangia A (2017) 7.03—Hydrogen bonding in molecular crystals. In: Atwood JL (ed) Comprehensive supramolecular chemistry II. Elsevier, Oxford, pp 25–48. https://doi.org/10.1016/B978-0-12-409547-2.12598-3

Affiliations

Denise Böck[1] · Andreas Beuchel[1] · Richard Goddard[2] · Peter Imming[1] · Rüdiger W. Seidel[1]

[1] Martin-Luther-Universität Halle-Wittenberg, Institut für Pharmazie, Wolfgang-Langenbeck-Str. 4, 06120 Halle (Saale), Germany

[2] Max-Planck-Institut für Kohlenforschung, Kaiser-Wilhelm-Platz 1, 45470 Mülheim an der Ruhr, Germany